Published October 12, 2009

Activation and desensitization of the olfactory cAMP-gated transduction channel: identification of functional modules

Clemens Waldeck, Kerstin Vocke, Nicole Ungerer, Stephan Frings, and Frank Möhrlen

Department of Molecular Physiology, University of Heidelberg, 69120 Heidelberg, Germany

Olfactory receptor neurons respond to odor stimulation with a receptor potential that results from the successive activation of cyclic AMP (cAMP)-gated, Ca^{2+}-permeable channels and Ca^{2+}-activated chloride channels. The cAMP-gated channels open at micromolar concentrations of their ligand and are subject to a Ca^{2+}-dependent feedback inhibition by calmodulin. Attempts to understand the operation of these channels have been hampered by the fact that the channel protein is composed of three different subunits, CNGA2, CNGA4, and CNGB1b. Here, we explore the individual role that each subunit plays in the gating process. Using site-directed mutagenesis and patch clamp analysis, we identify three functional modules that govern channel operation: a module that opens the channel, a module that stabilizes the open state at low cAMP concentrations, and a module that mediates rapid Ca^{2+}-dependent feedback inhibition. Each subunit could be assigned to one of these functions that, together, define the gating logic of the olfactory transduction channel.

INTRODUCTION

Recent studies of olfactory information processing in rodents have revealed that the detection and discrimination of odorants is a very fast process, completed within a few hundred milliseconds after contact with the odor (Abraham et al., 2004; Rinberg et al., 2006; Wesson et al., 2008a,b, 2009; Carey et al., 2009). This exciting finding has focused the attention on rapid transduction processes in olfactory receptor neurons (ORNs), in particular on the fast regulation of the olfactory cAMP-gated transduction channels. Olfactory transduction takes place in the sensory cilia of ORNs, which expose odorant receptor proteins to the inhaled air (for review see Kleene, 2008). When odors bind to these receptors, they trigger a transduction cascade that begins with the activation of adenylyl cyclase III and the synthesis of cAMP. The transduction channels in the ciliary membrane belong to the family of mammalian CNG cation channels that comprises seven proteins (CNGA1–A4, CNGB1a, CNGB1b, and CNGB3) (Craven and Zagotta, 2006; Biel and Michalakis, 2009). In photoreceptors and in ORNs, these proteins coassemble in various combinations to form heterotetrameric transduction channels, in particular A1-A1-A1-B1a in rod photoreceptors (Weitz et al., 2002; Zheng et al., 2002; Zhong et al., 2002), A3-A3-B3-B3 in cone photoreceptors (Peng et al., 2004), and A2-A2-A4-B1b in ORNs (Zheng and Zagotta, 2004). The basic functional properties of CNG channels are quite well understood (Biel and Michalakis, 2009). However, olfactory-specific channel properties, which result from the unique subunit combination of the channel in ORN cilia, are much less clear. For instance, although all subunit combinations are highly sensitive to cGMP, only the combination expressed in ORNs shows high cAMP sensitivity as well. This enables the olfactory A2-A2-A4-B1b channel to respond to micromolar concentrations of cAMP. In contrast, the photoreceptor channels are gated by cGMP, and cAMP is only a partial agonist for these channels (Altenhofen et al., 1991; Varnum et al., 1995).

A recent kinetic study has yielded a gating model that explains how olfactory CNG channels are opened by cAMP (Biskup et al., 2007). This model (the C4L model) was based on simultaneous measurements of ligand binding and the resulting gating activity, and it provides a suitable blueprint for the exploration of the channel machinery. The C4L model indicates that the four channel subunits are liganded sequentially. The second binding step basically opens the channel, and the two further liganding steps stabilize the open state. This novel gating concept describes the observed activation kinetics satisfactorily. However, it leaves open the question of which of the four subunits are responsible for channel opening, and which subunits stabilize the open channel. Here, we provide answers to these questions using a mutagenesis approach in heterologously expressed rat A2-A2-A4-B1b channels.

Correspondence to Stephan Frings: s.frings@zoo.uni-heidelberg.de

Abbreviations used in this paper: BADAN, 6-bromoacetyl-2-dimethylaminonaphthalene; ORN, olfactory receptor neuron; YFP, yellow fluorescent protein.

The Rockefeller University Press $30.00
J. Gen. Physiol. Vol. 134 No. 5 397–408
www.jgp.org/cgi/doi/10.1085/jgp.200910296

Supplemental Material can be found at:
/content/suppl/2009/10/12/jgp.200910296.DC1.html

Published October 12, 2009

The cAMP sensitivity of its transduction channels plays a pivotal role in ORN function. One reason is that odor-induced cAMP synthesis works with low efficiency and cAMP reaches only low micromolar concentrations during the first few hundred milliseconds of odor stimulation (Bhandawat et al., 2005; Takeuchi and Kurahashi, 2005), the time period that is critical for odor detection and discrimination (Wesson et al., 2008a; Carey et al., 2009). This is, however, sufficient for A2-A2-A4-B1b channels, which require only ∼5 µM cAMP for half-maximal activation and thus ensure chemo-electrical transduction even upon weak stimulation. Another important aspect results from the fact that the channels are highly Ca^{2+} permeable. During odor stimulation, Ca^{2+} enters the cilia and triggers a negative feedback mechanism that decreases the channels' cAMP sensitivity (Chen and Yau, 1994; Kurahashi and Menini, 1997). This desensitization is completed within <1 s (Bradley et al., 2004), and it curtails the receptor current and determines the response dynamics of the ORN (Song et al., 2008). Thus, the sensitivity of A2-A2-A4-B1b channels to cAMP is a tunable key parameter for the odor response in ORNs. Here, we examine the role that each subunit type plays in cAMP-dependent activation of A2-A2-A4-B1b channels by selectively disabling the cAMP-binding site of each subunit. This mutagenesis approach aims to clarify which of the subunits binds cAMP and how cAMP binding contributes to channel gating.

Mechanistic explanations of the rapid, Ca^{2+}-dependent channel desensitization are still unsatisfactory. The Ca^{2+} effect is thought to be mediated by calmodulin, for which each of the three subunits has at least one binding site. A study of A2-A2-A4-B1b channels in excised patches from which endogenous calmodulin was removed ("washed channels") revealed that calmodulin requires two distinct interaction sites with the channels to induce rapid desensitization (Bradley et al., 2004). These were identified as LQ-type calmodulin-binding sites on CNGA4 and CNGB1b. Calmodulin is permanently associated with the channel, even at low Ca^{2+} concentrations in the resting cell ($[Ca^{2+}]_i \leq 0.1$ µM), without affecting cAMP sensitivity. Upon stimulation of the ORN, a rise of $[Ca^{2+}]_i$ to ≥1 µM induces desensitization and, hence, inhibits channel activity. Although these results demonstrated that calmodulin is pre-associated with the A2-A2-A4-B1b channel as a Ca^{2+} sensor, they did not reveal the individual functions of each of the two LQ sites. A recent mutagenesis study identified CNGB1b as the regulatory target for desensitization (Song et al., 2008). We find that the CNGB1b calmodulin-binding site is necessary and sufficient for rapid desensitization if endogenous calmodulin is left attached to the channel. A biochemical examination of this site revealed that it is able to interact both with the C terminus and with the N terminus of calmodulin. Its ability to bind to either lobe of calmodulin is critical for desensitization. Contrary to expectations, the CNGA4 subunit appears not to be involved in this process. Our results thus assign specific functions to each of the three subunit types that coassemble in the native olfactory transduction channel, and we identify their specific contributions to activation and desensitization of the channel.

MATERIALS AND METHODS

Site-directed mutagenesis and transient expression of CNG channel subunits

Expression of cloned cDNAs encoding the CNGA2, CNGA4, and CNGB1b subunits in HEK 293 cells was either done with Ca^{2+} phosphate–mediated transfection and performed as described previously (Bönigk et al., 1999), or with TransFectin (Bio-Rad Laboratories) and Nucleofector I (Lonza) according to the manufacturers' instructions. Expression vectors were created by subcloning the coding region, including the 5′ untranslated region (Qu et al., 2006) from pCIS (CNGA2 and CNGA4; provided by J. Bradley, Université Paris Descartes, Paris, France) and pcDNAI-amp (CNGB1b; provided by W. Bönigk, Institut für Strukturbiologie und Biophysik, Jülich, Germany) into pcDNA3.1 (Invitrogen). Site-directed mutagenesis was performed using the Quick Change II XL Site-Directed Mutagenesis kit (Agilent Technologies) according to the manufacturer's instructions, and all constructs were sequenced before functional assays. The following amino acids were targeted for mutagenesis: R538E (CNGA2), R430E (CNGA4), R657E (CNGB1b), L292E (CNGA4), and L183E (CNGB1b). As a reporter for transfection efficiency and CNG subunit expression (wild type and mutants), recombinant fusion genes carrying C-terminal fluorescent protein tags were generated. CNGA2 was subcloned in pEYFP-N1 (Takara Bio Inc.). To ensure similar expression levels of $CNGA2^{YFP}$ in our experiments, we measured the yellow fluorescent protein (YFP) fluorescence of each cell using standardized imaging settings and divided the cells into four classes according to their fluorescence intensity (Fig. S3). For our experiments, we used only class 4 cells, which had the highest expression level. To increase the gain of A2-A2-A4-B1b coassembly in the desensitization experiments, we constructed a dual expression plasmid that encoded both CNGA4 and CNGB1b. Moreover, CNGA4 was tagged with red fluorescent protein (RFP), and CNGB1b was tagged with cyan fluorescent protein (CFP) in this vector. For this purpose, mRFP1-Q66T (provided by T. Kuner, University of Heidelberg, Heidelberg, Germany) was inserted into CNGA4/pcDNA3.1. ECFP (from pECFP-C1; Takara Bio Inc.) was inserted into CNGB1b/pcDNA3.1. Simultaneous transient expression of CNGA4 and CNGB1b subunits was enhanced by subcloning CNGA4/RFP and CNGB1b/CFP coding fragments into the pBudCE4.1 (Invitrogen) transfection plasmid. Cotransfection of this construct with CNGA2 allowed us to specifically select those cells that expressed all three subunits for patch clamp recording. Because CNGA4 and CNGB1b do not form functional channels by themselves, each transfected cell that did show cAMP-dependent current, as well as cyan and red fluorescence, was identified to express all three subunits.

Electrophysiology

For inside-out patches, the pipette solution contained (in mM) 140 NaCl, 3 KCl, 10 EGTA, and 10 HEPES, pH 7.4, NaOH. The bath solution was the pipette solution without EGTA, plus 2.5 mM $CaCl_2$ and 1 mM $MgCl_2$. Test solutions were the pipette solution with 10 mM HEDTA instead of EGTA and 8.5 mM $CaCl_2$ to obtain a free Ca^{2+} concentration $[Ca^{2+}]$ of 20 µM. $[Ca^{2+}]$ was calculated using WINMAXC v2.50 (Patton et al., 2004) and verified using a

Published October 12, 2009

Ca^{2+}-sensitive electrode (KwiKCal; WPI). The electrode was calibrated with the CalBuf-1 set of Ca^{2+} buffers (WPI) before each measurement. To construct dose–response curves, cAMP-dependent currents were recorded at −50 mV and fitted by a Hill equation,

$$I/I_{max} = c^n/\left[c^n + K_{1/2}^n\right], \quad (1)$$

where c is the cAMP concentration and n is the Hill coefficient. Dose–response curves were fitted separately for each patch. For the figures, curves were constructed from the mean values of $K_{1/2}$ and n obtained from these fits, and are presented together with the mean I/I_{max} values (±SD) for each cAMP concentration. The maximal current amplitudes are the mean values at −50 mV (± SD). To induce desensitization by experimentally applied calmodulin, the inside-out patch was washed for 10 min in 10 mM EGTA. The channels were activated to an initial open probability of 0.7–0.9 by 10 µM cAMP (A2-A2-A4-B1b), 30 µM cAMP (A2-A2-A2-A4), or 100 µM cAMP (A2-A2-A2-B1b). To induce desensitization, 0.5 µM calmodulin and 150 µM Ca^{2+} were co-applied using a rapid perfusion system, according to published protocols (50–300 µM Ca^{2+}) (Bradley et al., 2001, 2004). For experiments with endogenous calmodulin, the inside-out patches were excised into the bath solution containing 2.5 mM Ca^{2+} to prevent calmodulin from dissociating from the CNG channels. After a brief exposure to Ca^{2+}-free solution, the channels were perfused with 20 µM Ca^{2+} and activated to an initial open probability of 0.7–0.9 by 15 µM cAMP (A2-A2-A4-B1b), 30 µM cAMP (A2-A2-A2-A4), or 40 µM cAMP (A2-A2-A2-B1b). Relative currents, I_{rel}, were normalized to the maximal current amplitude at the respective cAMP concentration. To compare the time courses of calmodulin action, the current was normalized (I_{norm}) to the amplitude of maximal current suppression by calmodulin, ΔI_{CaM}. Accordingly, $I_{norm}(t) = I_{CaM(t)}/\Delta I_{CaM}$, where $I_{CaM(t)}$ is the calmodulin-sensitive part of the current. All plots of $I_{norm}(t)$ run from unity to zero. Unity marks the mean cAMP-induced current before the addition of exogenous Ca^{2+} calmodulin (or the addition of Ca^{2+} to endogenous calmodulin); zero represents the residual steady-state cAMP-dependent current after desensitization had fully developed. For experimentally applied calmodulin, the time course of current decline was best described by the sum of two exponentials:

$$I_{norm}(t) = a_f e^{-\frac{t}{\tau_{fast}}} + \left(1 - a_f\right) e^{-\frac{t}{\tau_{slow}}}. \quad (2)$$

τ_{fast} and τ_{slow} describe the fast and the slow components of current decline, and a_f represents the relative contribution of the fast component. For experiments with endogenous calmodulin, the time course of current decline was best described by a single exponential,

$$I_{norm}(t) = e^{-\frac{t}{\tau}}.$$

For the kinetic analysis, we compared τ_{fast} for exogenous calmodulin with τ for endogenous calmodulin.

Synthesis and 6-bromoacetyl-2-dimethylaminonaphthalene (BADAN) labeling of peptides

Peptide synthesis and labeling were performed at Peptide Specialty Laboratories GmbH. The peptides represent the LQ-type calmodulin-binding site of the CNGB1b subunit (Bradley et al., 2004), corresponding to amino acid residues 177–202 (GenBank accession no. AF068572) and carrying a C-terminal cysteine residue for labeling. Wild-type and L183E substitution (Bradley et al., 2004) were synthesized using Fmoc chemistry solid-phase peptide synthesis. Peptides were deprotected and cleaved from the resin with 25% piperidine in DMF, 95% TFA, 4% triethylsilane, and 1% water, respectively. Purification was performed by reverse-phase HPLC on a C-18 column (Gemini; Phenomenex) with an acetonitrile/TFA gradient. Site-directed fluorescence labeling with BADAN (Owenius et al., 1999) was performed in the dark overnight at 4°C using a 10-fold molar excess of label over peptide. Reaction buffer was 1 ml of 20 mM Tris, pH 7.4, supplemented with 200 µl BADAN in DMF. The product was purified by reverse-phase HPLC (see above), to remove unlabeled peptide, and lyophilized. Its homogeneity was confirmed by MALDI mass spectroscopy.

Preparation of calmodulin

Calmodulin wild-type protein was purchased from EMD. Plasmid vectors for expression of calmodulin mutants (Peterson et al., 1999) were provided by D.T. Yue (John Hopkins University School of Medicine, Baltimore, MD). In these constructs (CaM^{12}, CaM^{34}, and CaM^{1234}) EF-hand calcium-binding sites were disabled by D→A exchange (Keen et al., 1999). Expression vectors were created by subcloning the NdeI/BamHI fragments into pET-28a(+) (EMD). This resulted in N-terminally His_6-tagged fusion proteins. After expression in *Escherichia coli* BL21 (DE3) pLysS and purification on a His Trap FF column (GE Healthcare), His_6–calmodulin constructs were subjected to SDS-PAGE to assure homogeneity, or dialyzed against distilled water and lyophilized. To assure a native conformation of the proteins after dissolving in buffer A (see below), circular dichroism measurements were performed.

Fluorescence measurements

Steady-state fluorescence with BADAN was measured (Owenius et al., 1999; Kipp et al., 2002) with a spectrofluorometer (LS50; PerkinElmer) in quartz cuvettes (Hellma) containing a total volume of 100 µl. Fluorescence emission spectra were recorded at 400–600 nm after excitation at 387 nm (bandwidth for excitation and emission, 5–10 nm; scan speed, 200 nm/min). Stock solutions of labeled peptide (0.15 mM) and calmodulin (0.3 mM) were made in buffer A (20 mM Tris, 100 mM NaCl, and 10 mM EGTA, pH 7.2). Peptide concentrations were determined spectrophotometrically based on the molar absorptivity of the BADAN group at 386 nm: $\varepsilon_{386\,nm} = 20{,}100\ M^{-1}\ cm^{-1}$. Calmodulin concentrations were determined by Bradford assay. The final concentration of all samples was held at 1.5 µM for labeled peptides (CNGB1b and $CNGB1b^{L183E}$) and 3.0 µM for calmodulin (CaM, CaM^{12}, CaM^{34}, and CaM^{1234}). Spectra were recorded in the presence or absence of calmodulin in various free Ca^{2+} concentrations, which were generated by different ratios of buffer A and buffer B (buffer A supplemented with 10 mM Ca^{2+}) (Williams and Fay, 1990). The free Ca^{2+} concentration was calculated using the WINMAXC v2.50 free metal calculation program (Patton et al., 2004).

Online supplemental material

The supplemental material contains detailed information on the selection of A2-A2-A4-B1b channels in patch clamp experiments (Figs. S1 and S2), the classification of expression levels in HEK 293 cells (Fig. S3), the protocols for exploring the effects of exogenous and endogenous calmodulin (Fig. S4), and the fluorescence readout of labeled binding-site peptides (Fig. S5). Figs. S1–S5 are available at http://www.jgp.org/cgi/content/full/jgp.200910296/DC1.

RESULTS

We expressed CNGA2, CNGA4, and CNGB1b in HEK 293 cells and determined the cAMP sensitivity of the resulting channels in excised patches. We selected membrane patches that contained >90% properly assembled

Published October 12, 2009

A2-A2-A4-B1b channels using the cAMP sensitivity and its voltage dependence as well as the Hill coefficient as indicators for correct channel assembly. This selection was possible because all other functional combinations of the three subunit types produced channels that differed significantly in these parameters (details in Figs. S1 and S2). We used these criteria to identify patches with >90% A2-A2-A4-B1b channels: (1) The ratio of activation constants $K_{1/2}^{cAMP}$ at −50 mV and +50 mV, $K_{1/2}^{-50}/K_{1/2}^{50}$, was >1.33 (Fig. S1), or (2) the fractional current I/I_{max} at the subsaturating cAMP concentration of 3.4 µM is >0.31 (Fig. S2).

The role of each subunit type in channel activation

To identify the specific functional role of each subunit type in channel activation, we selectively rendered the cAMP-binding site in each subunit inoperative by site-directed mutagenesis and analyzed the consequence of this perturbation for channel function. CNGA2, CNGA4, and CNGB1b possess similar cyclic nucleotide–binding sites located in the intracellular C-terminal part of the proteins (for reviews see Kaupp and Seifert, 2002; Craven and Zagotta, 2006; Biel and Michalakis, 2007). Conserved within the binding sites of all CNG channels is an arginine residue that forms an electrostatic bond with the cyclized phosphate of cAMP or cGMP. These residues are R^{538} in CNGA2 (Dhallan et al., 1990), R^{430} in CNGA4 (Bradley et al., 1994; Liman and Buck, 1994), and R^{657} in CNGB1b (Sautter et al., 1998; Bönigk et al., 1999) (Fig. 1 A). If the corresponding arginine in the photoreceptor channel subunit CNGA1 is replaced by a glutamate (R559E), the ligand sensitivity of the mutant is reduced by a factor of 10,000 (Tibbs et al., 1998). We used this observation to selectively prevent cAMP binding to each subunit type. To monitor the expression efficiency in these experiments, we tagged the CNGA2 subunit with YFP (see Materials and methods) and selected cells of similar shape, similarly high fluorescence intensity (class 4 cells; Fig. S3), and similar levels of $CNGA2^{YFP}$ expression. Three parameters were evaluated to ensure that the mutant subunits were coassembled in A2-A2-A4-B1b stoichiometry in these experiments: the cAMP concentration for half-maximal activation, its voltage dependence, and the Hill coefficient of the dose–response relation. In this way, it was possible to distinguish channels containing three different subunits from those with one or two subunits (legend to Fig. 1). Current–voltage relations of wild-type and mutant A2-A2-A4-B1b were recorded at different cAMP concentrations (Fig. 1 B), and the maximal cAMP-dependent current, I_{max}, was

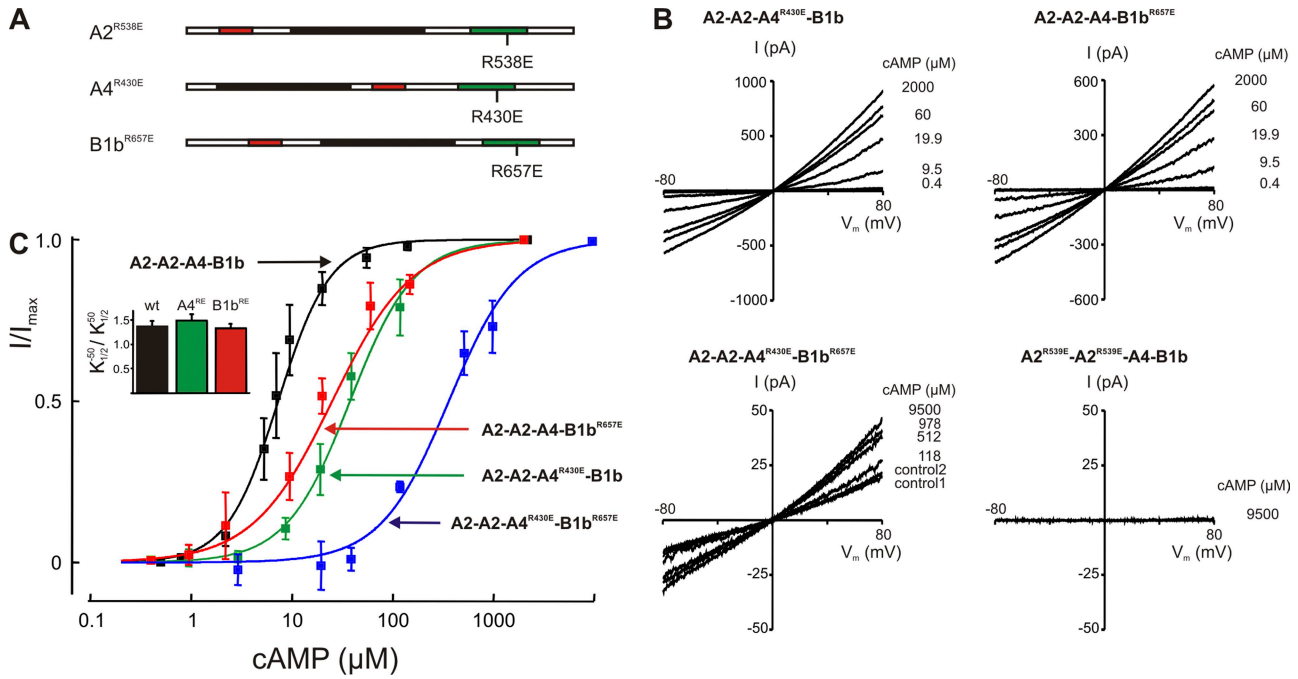

Figure 1. Channel activation. (A) Schematic drawing of the three polypeptides that coassemble in the A2-A2-A4-B1b channel, indicating the position of R/E mutations that were introduced to disable cAMP binding. The black sections represent the six transmembrane domains of each subunit, the cAMP-binding sites are depicted green, and the calmodulin-binding sites are shown in red. (B) I/V_m relations illustrating experiments designed to determine the cAMP sensitivity. The applied cAMP concentration is depicted to the right of each current trace. Selection parameters for A2-A2-A4-B1b channels were: (1) $K_{1/2}^{-50}/K_{1/2}^{50} > 1.3$; (2) $K_{1/2}$ different from 30 µM (A2-A2-A2-B1b) or 10 µM (A2-A2-A2-A4); and (3) Hill coefficient different from 1.8. (C) Contribution of subunits to cAMP sensitivity. The cAMP dose–response relation for wild-type A2-A2-A4-B1b channels was fitted with $K_{1/2} = 7.3 \pm 1.7$ µM, $n = 1.71 \pm 0.3$ (black). Mutant channels yielded the following fit parameters: A2-A2-$A4^{R430E}$-B1b: $K_{1/2} = 37.6 \pm 8.5$ µM, $n = 1.37 \pm 0.2$ (green); A2-A2-A4-$B1b^{R657E}$: $K_{1/2} = 25.5 \pm 10.5$ µM, $n = 1.10 \pm 0.1$ (red); and A2-A2-$A4^{R430E}$-$B1b^{R657E}$: $K_{1/2} = 359.5 \pm 68.5$ µM, $n = 1.28 \pm 0.2$ (blue).

Published October 12, 2009

determined at 2 or 9.5 mM cAMP and −50 mV. We first asked whether the channels remained functional when CNGA4 or CNGB1b was incapacitated by an R/E mutation. Excised patches from cells expressing wild-type A2-A2-A4-B1b channels had a mean I_{max} of 423 ± 296 pA. Although only cells with high protein expression were selected (class 4 cells; Fig. S3), channel densities varied considerably between individual patches, giving rise to a range of I_{max} amplitudes. The maximal patch current from cells expressing single-mutant channels was 264 ± 252 pA (A2-A2-A4^{R430E}-B1b) and 119 ± 85 pA (A2-A2-A4-B1b^{R657E}). This observation demonstrates qualitatively that the mutant channels were activated by cAMP. We next asked whether the channels were operative when only CNGA2 could bind cAMP. Cotransfection of CNGA2 with both CNGA4^{R430E} and CNGB1b^{R657E} resulted in 50-fold lower current levels (Fig. 1 B; 13 ± 2 pA; 3 out of 12 patches), suggesting that the maximal open probability of the A2-A2-A4^{R430E}-B1b^{R657E} channels is very low, but not zero. In contrast, when the R/E mutation was placed into the CNGA2 subunit, the resulting A2^{R538E}-A2^{R538E}-A4-B1b channels did not open, even at 9.5 mM cAMP, confirming that this subunit is indispensable for channel gating at micromolar cAMP concentrations.

For a quantitative evaluation of the mutant channel properties, we determined their dose–response relations by measuring the macroscopic current at a range of cAMP concentrations. Fig. 1 C illustrates the effect of the binding site mutations on the equilibrium cAMP sensitivity of the fully assembled channel. Introducing the R/E exchange into CNGA4 caused a shift of $K_{1/2}^{cAMP}$ from 7.3 µM to 37.6 ± 8.5 µM (five patches; Fig. 1 C, green). Mutating the CNGB1b-binding site had a similar effect, with $K_{1/2}^{cAMP}$ = 25.5 ± 10.5 µM (five patches; Fig. 1 C, red). These results show that the R/E mutation in the cAMP-binding sites of CNGA4 or CNGB1b caused a comparable reduction of cAMP sensitivity, as observed when the respective subunits were entirely omitted from the channel (A2-A2-A2-A4, $K_{1/2}^{cAMP}$ = 10 µM; A2-A2-A2-B1b, $K_{1/2}^{cAMP}$ = 30 µM) (Bönigk et al., 1999). In channels containing both mutants (A2-A2-A4^{R430E}-B1b^{R657E}), the dose–response relation was shifted to extremely high cAMP concentrations. Currents were too small in most patches to allow reliable dose–response analyses. However, the cAMP sensitivity could be determined in three patches and yielded a mean $K_{1/2}^{cAMP}$ of 359.5 ± 68.5 µM (Fig. 1 C, blue), illustrating a drastically reduced ligand sensitivity in channels with only two functional binding sites.

Collectively, our results suggest (1) that the minimal condition for channel activity is the presence of a CNGA2 subunit; (2) that either of the two subunits CNGA4 and CNGB1b can, by itself, dramatically increase the efficiency of channel operation at high cAMP concentrations; and (3) that the liganding of a further subunit serves to stabilize the open state at low cAMP concentrations.

The role of CNGB1b in channel desensitization

It was reported earlier that the endogenous channel–calmodulin complex is relatively stable. When formed inside an ORN or an HEK 293 cell, it can only be dissociated by a prolonged (∼10-min) wash in Ca^{2+}-free solution (Lynch and Lindemann, 1994; Balasubramanian et al., 1996). In contrast, the complex formed by experimentally applied exogenous calmodulin disintegrates within seconds in the absence of Ca^{2+} (Fig. S4; Bradley et al., 2001, 2004). In view of this difference in stability, we reasoned that the endogenous complex may have structural features different from the exogenous complex. Because most available data originate from experiments with the exogenous complex, we tested this hypothesis by examining Ca^{2+}-induced desensitization with its endogenous Ca^{2+} sensor still attached to the channels. We assume that this Ca^{2+} sensor is calmodulin because a set of calmodulin-binding sites has been identified on the three subunits (Liu et al., 1994; Bönigk et al., 1999; Bradley et al., 2004), and robust Ca^{2+} calmodulin effects on the olfactory channel have been documented (Chen and Yau, 1994; Balasubramanian et al., 1996; Bradley et al., 2001; Zheng et al., 2003). The final proof of calmodulin association with the channel awaits in vivo binding assays.

One conspicuous difference between the endogenous complex and the exogenous complex occurred in the desensitization kinetics. As shown previously, channels lacking either CNGA4 or CNGB1b subunits responded very slowly when calmodulin was added to the excised patch, whereas A2-A2-A4-B1b channels responded rapidly (Bradley et al., 2001, 2004; Munger et al., 2001). Consistent with these findings, we observed that the application of 0.5 µM calmodulin to A2-A2-A4-B1b channels, from which endogenous calmodulin had been removed, induced a rapid current decline in the presence of 10 µM cAMP/150 µM Ca^{2+} (Fig. 2 A). This effect was caused by a decrease of cAMP sensitivity, as $K_{1/2}^{cAMP}$ was shifted from 7.5 ± 0.5 to 20.0 ± 3.6 µM (four patches) upon the addition of Ca^{2+} calmodulin. Channels lacking CNGA4 responded much slower; it took 20-fold more time to reach 50% of the current decline (Fig. 2 A and Fig. S4). Thus, as shown previously (Bradley et al., 2001, 2004; Munger et al., 2001), CNGA4 is necessary for rapid desensitization by exogenous calmodulin. In contrast, channels with their endogenous calmodulin still attached responded rapidly to the application of 20 µM Ca^{2+}, even in the absence of CNGA4 (Fig. 2 A, right). Kinetic analysis of the normalized calmodulin response ($I_{norm}(t) = I_{CaM(t)}/\Delta I_{CaM}$; see Materials and methods) revealed that the time course of current decline was similarly rapid in the presence and the absence of CNGA4, provided the channels used its endogenous calmodulin as Ca^{2+} sensor (Fig. 2 B). This observation points to a marked difference between channel regulation by endogenous calmodulin and regulation by experimentally added calmodulin.

Published October 12, 2009

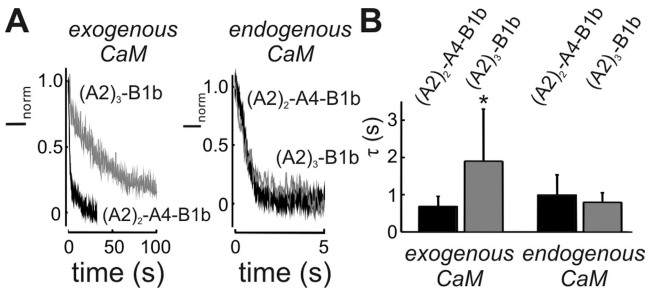

Figure 2. Ca^{2+}-dependent desensitization. (A) Current decline in patches expressing either A2-A2-A4-B1b channels (black) or with channels that lack the CNGA4 subunit (A2-A2-A2-B1b; gray) upon exposure to Ca^{2+}. The current decline reflects the time course of the desensitization process (see also Fig. S4). Desensitization is fast in A2-A2-A4-B1b channels with endogenous and exogenous calmodulin (black). Channels without CNGA4 desensitize slowly with exogenous calmodulin (left, gray), but rapidly with endogenous calmodulin (right, gray; note the different time scale). (B) Summary of the desensitization kinetics in A2-A2-A4-B1b channels and in channels lacking CNGA4. The time constant of current decline dependent on CNGA4 only in the exogenous complex (channel with CNGA4: τ_{fast} = 0.7 ± 0.3 s and a_f = 0.68 ± 0.23, seven patches; channel without CNGA4: τ_{fast} = 1.9 ± 1.4 s and a_f = 0.44 ± 0.16, 10 patches). Desensitization speed in the endogenous complex did not depend on CNGA4 (channels with CNGA4: τ = 0.9 ± 0.5 s, five patches; channels without CNGA4: τ = 0.8 ± 0.3 s, four patches).

To closer examine this disparity, we selectively disabled the calmodulin-binding sites of CNGA4 and CNGB1b by mutagenesis and tested the consequences for channel regulation by endogenous calmodulin. The LQ-type binding motifs L^{292}QHVNKRLERR in the C-terminal region of CNGA4 (Bradley et al., 2004) and L^{183}QELVKMFKER in the N-terminal region of CNGB1b (Weitz et al., 1998) were subjected to an L/E exchange ($A4^{L292E}$ and $B1b^{L183E}$; Fig. 3 A). These mutations were previously shown to prevent the desensitization of channels by exogenous calmodulin (Bradley et al., 2004). Unlike the removal of an entire subunit type, the introduction of L/E point mutations into CNGA4 and CNGB1b did not change the cAMP sensitivity in the absence of Ca^{2+} (Bradley et al., 2004). We were, therefore, able to use the cAMP sensitivity as criterion to identify patches with appropriately assembled channels. All patches used for these experiments displayed an I/I_{max} value of >0.31, with a test solution containing 3.4 µM cAMP (Fig. 3 D, inset). I/V_m relations were recorded to determine the cAMP sensitivity (Fig. 3, B and C). In the presence of 20 µM Ca^{2+}, wild-type A2-A2-A4-B1b channels with endogenous calmodulin showed a reduced cAMP sensitivity (Fig. 3 D, black). The $K_{1/2}^{cAMP}$ was shifted to 47.8 ± 4.4 µM (seven patches). The same dose–response relation was observed with A2-A2-$A4^{L292E}$-B1b channels exposed to Ca^{2+}, with a $K_{1/2}^{cAMP}$ of 46.9 ± 12 µM (five patches; Fig. 3 D, green). In contrast, the cAMP sensitivity of A2-A2-A4-$B1b^{L183E}$ channels was virtually unchanged by Ca^{2+} ($K_{1/2}^{cAMP}$: 10.8 ± 3.2 µM; five patches; Fig. 3 D, red). This value does not deviate significantly from the sensitivity of wild-type A2-A2-A4-B1b channels measured without Ca^{2+} ($K_{1/2}^{cAMP}$ = 7.3 ± 1.2 µM;

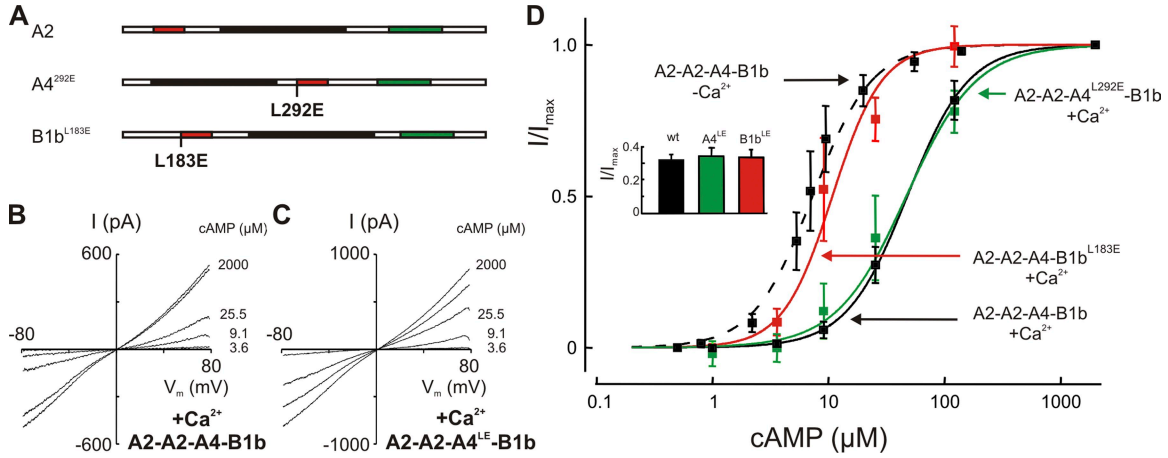

Figure 3. CNGB1b mediates Ca^{2+}-dependent desensitization. (A) Schematic representation of the three channel subunits indicating the locations of point mutations designed to disable calmodulin-mediated feedback inhibition. (B) I/V_m relations obtained from a patch containing wild-type A2-A2-A4-B1b channels with its endogenous calmodulin recorded in the presence of 20 µM Ca^{2+}. $K_{1/2}^{-50}$ / $K_{1/2}^{50}$ was 1.31. (C) A similar I/V_m relation obtained from A2-A2-$A4^{L292E}$-B1b channels indicates that CNA4 does not contribute to desensitization. $K_{1/2}^{-50}$ / $K_{1/2}^{50}$ was 1.34. (D) Dose–response relations of different subunit combinations tested with endogenous calmodulin. Wild-type A2-A2-A4-B1b channels responded to 20 µM Ca^{2+} with reduced cAMP sensitivity: $K_{1/2}$ increased from 7.3 ± 1.7 µM, n = 1.71 ± 0.3 at 0 Ca^{2+} (dashed line) to 47.8 ± 4.4 µM, n = 1.7 ± 0.3 at 20 µM Ca^{2+} (solid black line). A similar desensitization was observed with the A2-A2-$A4^{L292E}$-B1b channel: $K_{1/2}$ = 46.9 ± 12.0 µM, n = 1.4 ± 0.4 (green), illustrating that the calmodulin-binding site of CNGA4 is not required for desensitization. In contrast, A2-A2-A4-$B1b^{L183E}$ channels did not desensitize in the presence of Ca^{2+} ($K_{1/2}$ = 10.8 ± 3.2 µM; n = 2.0 ± 0.8; red), demonstrating that CNGB1b is necessary and sufficient for desensitization in the endogenous complex. (Inset) Controls to document predominant A2-A2-A4-B1b expression in the patches used for these experiments. Measurements were performed with 3.4 µM cAMP. An I/I_{max} value >0.31 indicates >90% coassembly of A2-A2-A4-B1b channels in the patch. Values were 0.32 ± 0.03 (seven patches) for A2-A2-A4-B1b, 0.34 ± 0.05 (five patches) for A2-A2-$A4^{L292E}$-B1b, and 0.33 ± 0.04 (five patches) for A2-A2-A4-$B1b^{L183E}$.

Published October 12, 2009

seven patches). These results demonstrate that the LQ motif in CNGA4, which is essential for rapid desensitization by experimentally applied calmodulin (Bradley et al., 2004), does not participate in channel regulation when desensitization is mediated by endogenous calmodulin. The LQ motif of CNGB1b is necessary and sufficient for this process. As suggested earlier (Song et al., 2008), it represents the effector site for the allosteric regulation of cAMP sensitivity by calmodulin.

The calmodulin-binding site of CNGB1b

To closer examine the binding of calmodulin to the binding site of CNGB1b, we synthesized a 27-residue peptide consisting of the consensus motif (bold in the following sequence) and its immediate surroundings: AIINDR**L**^{183}**QELVKMFKER**TEKVKEKLIC. The fluorescent dye BADAN was covalently coupled to the C-terminal cysteine residue to allow the spectroscopic examination of calmodulin binding to this peptide (Fig. S5). We investigated the Ca^{2+} dependence of peptide–calmodulin interaction in a 1:2 molar ratio and found that binding occurred with high Ca^{2+} affinity. The dose–response relation yielded a $K_{1/2}^{Ca}$ of 12 nM for the binding of Ca^{2+} calmodulin to the B1b peptide (Fig. 4 A, ●). To examine the specificity of this interaction, we repeated the experiments with calmodulin mutants, in which the two N-terminal Ca^{2+}-binding sites (CaM^{12}), the two C-terminal binding sites (CaM^{34}), or all four sites (CaM^{1234}) were disabled by a D→A exchange (Peterson et al., 1999). CaM^{1234} did not bind to the peptide (Fig. 4 A, ○), whereas CaM^{12} and CaM^{34} both bound with a slightly reduced Ca^{2+} affinity ($K_{1/2}^{Ca}$ = 21–27 nm; Fig. 4 A, ▼ and ▲). Thus, in the peptide-binding assay, the N-terminal CNGB1b-binding site displays a high-affinity interaction with both Ca^{2+}-binding lobes of the calmodulin molecule. Because the L183E exchange in the CNGB1b subunit abolished the Ca^{2+}-dependent desensitization of the A2-A2-A4-$B1b^{L183E}$ channel (Bradley et al., 2004) (Fig. 3 D), we investigated the effect of this L/E exchange in the peptide–calmodulin binding assay. The corresponding peptide (AIINDR**E**^{183}**QELVKMFKER**TEKVKEKLIC) showed Ca^{2+}-dependent binding with reduced affinity ($K_{1/2}^{Ca}$ = 60 nM; Fig. 4 B, ●) to wild-type calmodulin, and no binding to the inactive CaM^{1234} mutant at any Ca^{2+} concentration tested (Fig. 4 B, ○). In contrast to the wild-type peptide, the L/E mutant also did not bind to CaM^{12} or CaM^{34} at any Ca^{2+} concentration (Fig. 4 B, ▼ and ▲). These peptide studies suggest that the B1b-binding site is able to interact both with the N-terminal and the C-terminal lobe of calmodulin, if Ca^{2+} is bound to that lobe, and that this binding requires the intact LQ motif. Collectively, our results support the hypothesis that the B1b-binding site in the A2-A2-A4-B1b channel triggers channel desensitization through Ca^{2+}-dependent interaction with one of the two Ca^{2+}-binding lobes of a calmodulin molecule.

DISCUSSION

Our results complement a series of studies on olfactory A2-A2-A4-B1b channels that have illustrated the coassembly of the three channel subunits in this particular CNG channel (Sautter et al., 1998; Bönigk et al., 1999), the subunit stoichiometry (Zheng and Zagotta, 2004), the channel's gating principle (Nache et al., 2005; Biskup et al., 2007), and the Ca^{2+}-dependent feedback regulation (Bradley et al., 2001, 2004; Munger et al., 2001; Trudeau and Zagotta, 2003). These and other studies (for reviews see Kaupp and Seifert, 2002; Matulef and Zagotta, 2003; Bradley et al., 2005; Craven and Zagotta, 2006; Pifferi et al., 2006; Biel and Michalakis, 2007) have clearly shown that A2-A2-A4-B1b channels operate at low micromolar cAMP concentrations, conduct Ca^{2+} efficiently, and are desensitized by Ca^{2+} calmodulin. To advance mechanistic concepts of the allosteric processes that lead from cAMP binding to activation and desensitization of the olfactory channel, we sought to identify the specific role that each subunit plays in channel activation and rapid desensitization.

Channel activation

Our mutagenesis study revealed that the function of CNGA2 is indispensable for channel function; channels containing inactive $CNGA2^{R538E}$ subunits did not open at micromolar cAMP concentrations. On the other hand,

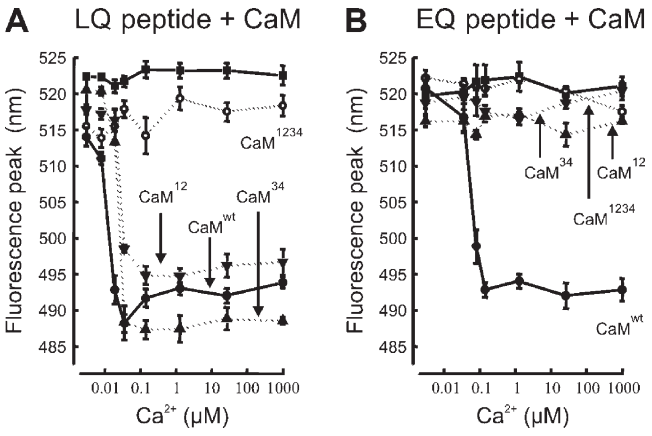

Figure 4. Calmodulin binding to CNGB1b. (A) Ca^{2+}-dependent binding of calmodulin to an LQ peptide representing the N-terminal calmodulin-binding site of CNGB1b. The peptide binds with a $K_{1/2}^{Ca}$ of 12 nM to wild-type calmodulin (CaM^{wt}, ●), with $K_{1/2}^{Ca}$ = 21 nM to the calmodulin mutant CaM^{12} (▲), and with $K_{1/2}^{Ca}$ = 27 nM to the mutant CaM^{34} (▼). The peptide produced neither a Ca^{2+}-dependent fluorescence signal by itself (■) nor in the presence of the inactive calmodulin mutant CaM^{1234} (○). (B) An L→E exchange that corresponds to the key position 183 of the CNGB1b subunit eliminates binding of the peptide to calmodulin with one disabled lobe. The EQ peptide binds wild-type calmodulin with a $K_{1/2}^{Ca}$ of 60 nM (CaM^{wt}, ●). However, no binding was observed with the calmodulin mutants CaM^{12} (▲) and CaM^{34} (▼), illustrating that the LQ site is necessary for the Ca^{2+}-dependent association of the CNGB1b peptide with partially liganded calmodulin.

Published October 12, 2009

CNGA2 can form cAMP-gated channels as a homomeric protein (Dhallan et al., 1990) or in combination with only one of the other subunits (Bradley et al., 1994; Liman and Buck, 1994; Sautter et al., 1998; Bönigk et al., 1999). Even when coassembled with inactive subunits (A2-A2-A4^{R430E}-B1b^{R657E}), CNGA2 could drive the channel into the open state, albeit with low efficacy. This observation firmly establishes CNGA2 as the principal subunit of the A2-A2-A4-B1b channel, responsible for the basic gating task, the opening of the channel pore.

The C4L model for channel activation (Biskup et al., 2007) specifies that the four channel subunits are liganded sequentially (Fig. 5 A). Our data provide insights into that sequence of cAMP binding and into the specific role of each subunit. We found that heteromeric channels can open when only two CNGA2 subunits are functional, but that they do not open when only CNGA4 and CNGB1b are functional. This observation suggests that the three subunits are not equivalent in the gating scheme, but that CNGA2 must be functional to allow channel opening. The critical step for channel opening in the C4L model is the binding of the second cAMP molecule. This drives the channel into the open state, which can then be stabilized by further cAMP binding. Our results suggest that only CNGA2 can serve as receptor for the second cAMP, and neither CNGA4 nor CNGB1b can substitute. Consequently, A2^{R538E}-A2^{R538E}-A4-B1b channels never open because the second cAMP cannot bind without intact CNGA2. The first binding step presumably involves CNGA4, as the cAMP-binding domain of this subunit confers high cAMP sensitivity to heteromeric channels (Shapiro and Zagotta, 2000). In this scenario, the CNGA4 subunit provides singly liganded channels at low cAMP concentrations, which can then be opened by CNGA2 upon binding of the second cAMP. The remaining two subunits serve to keep the channel open.

Studies of activation kinetics at low cAMP concentrations in CNA2 homomers and in A2-A2-A4-B1b channels revealed that a negative cooperativity effect reduces the stability of the doubly liganded state (Nache et al., 2005). Our data are consistent with this finding. We found an extremely low cAMP sensitivity in channels with only two intact subunits (A2-A2-A4^{R430E}-B1b^{R657E}). Our data also indicate that these mutant channels have a reduced open probability, as the maximal patch current at saturating cAMP concentrations is 50-fold smaller than in channels with three or four intact cAMP-binding sites. These observations are consistent with the prediction from the C4L model that the second binding step is not stable by itself. The second cAMP readily dissociates, hence limiting the maximal open probability. As the A2-A2-A4^{R430E}-B1b^{R657E} channel cannot reach a triply liganded state, a robust open conformation cannot be attained at micromolar cAMP concentrations. Clearly, a third liganding step is required to transfer the channel into a more stable open conformation. Our data show that this third binding step can be mediated equally well by CNGB1b and by the second CNGA2 subunit. Either subunit allows the channel to reach high levels of open

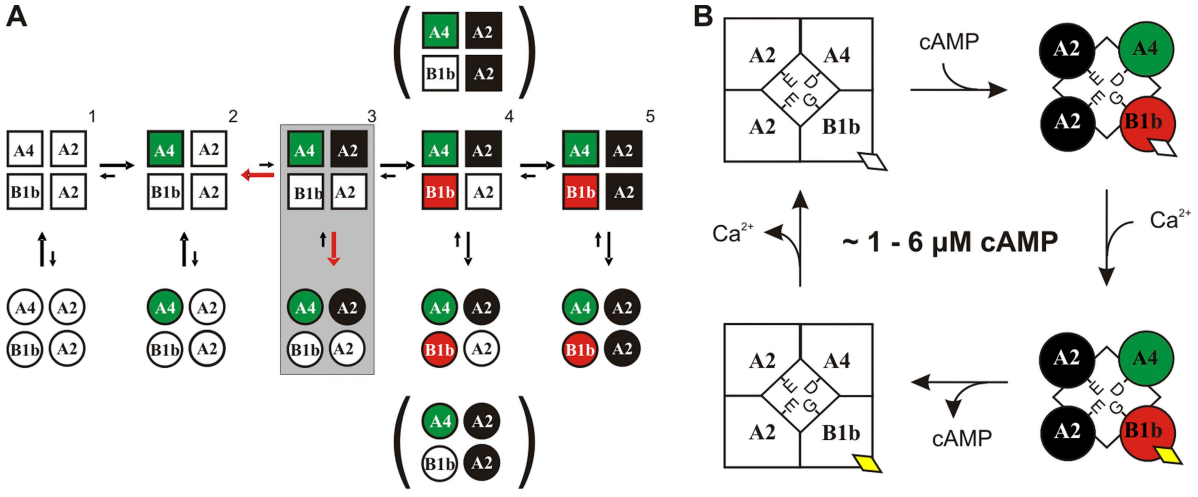

Figure 5. Activation and desensitization of olfactory cAMP-gated channels. (A) Activation. Graphic representation of the C4L gating model according to Biskup et al. (2007) with identified contributions of individual channel subunits. Squares depict closed states, and circles represent open states of the channel. The subunit with the highest cAMP affinity, CNGA4, may bind the first cAMP molecule, and one CNGA2 subunit must bind the second. Filled signals indicate cAMP-liganded subunits. The arrow sizes represent preferred gating transitions. The red arrows in the shaded box around the doubly liganded state 3 indicate that opening transitions compete with the loss of one cAMP, whose dissociation is favored by a negative cooperativity effect. The binding of cAMP to the second CNGA2 and to CNGB1b (states 4 and 5) drives the channel to high levels of open probability at low cAMP concentrations. (B) Desensitization. The channel mostly operates at 1–6 µM cAMP with open probabilities <50%. In this state of weak activation, the binding of Ca^{2+} to the endogenous calmodulin (diamonds) causes channel closure, as the interaction of Ca^{2+} calmodulin with CNBGB1b reduces the cAMP sensitivity. The channel remains in this desensitized state until Ca^{2+} is extruded from the cilia.

Published October 12, 2009

probability, provided that ~100 µM cAMP is applied. The need for such high cAMP concentrations in the channel with three cAMP-binding sites reflects the lack of the final binding step. If the fourth subunit binds cAMP, an open conformation is reached that is stable even at 10-fold lower cAMP concentrations. The fully liganded channel can open at 1–6 µM cAMP, a concentration reached in the cilia during the odor response. Collectively, our results can be adequately interpreted in the context of the C4L scheme. They corroborate and expand the C4L model by correlating individual subunit types with discrete liganding steps.

Ca^{2+}-dependent desensitization

There are several distinct modes of interaction between the cAMP-gated channel and calmodulin. Homomeric A2-A2-A2-A2 channels are desensitized by exogenous Ca^{2+} calmodulin through binding to an N-terminal domain (Chen and Yau, 1994; Liu et al., 1994). This interaction interferes with the intramolecular effect of an auto-excitatory domain that promotes gating efficacy (Trudeau and Zagotta, 2003). A different mechanism appears to desensitize A2-A2-A4-B1b channels challenged with exogenous calmodulin. Without a contribution of the CNGA2 subunit, two LQ-type calmodulin-binding sites on CNGA4 and CNGB1b mediate channel desensitization (Bradley et al., 2004). A third mode of channel regulation is at work when the channel is associated with its endogenous Ca^{2+}-binding protein, which we supposed to be calmodulin. This mode absolutely depends on CNGB1b, but it does not necessarily involve CNGA4. These observations make it very clear that channel regulation should be studied as close to the in vivo situation as possible, and they point out the prominent role of CNGB1b in this process.

Previous work has shown that the CNGB1b subunit increases Ca^{2+} permeation in the cAMP-gated channel, a consequence of the reduced stability of Ca^{2+} coordination within the pore of the heteromeric channel (Dzeja et al., 1999). Ca^{2+} ions are specifically coordinated by negatively charged intrapore residues (E^{342} in CNGA2 and D^{234} in CNGA4) (Bradley et al., 1994). CNGB1b, however, carries an uncharged glycine residue in the homologous position of its pore-lining domain (G^{463}; Bönigk et al., 1999), which weakens Ca^{2+} binding, shortens the dwell time of Ca^{2+} ions within the pore, and promotes Ca^{2+} permeation. Thus, one functional property that can be specifically assigned to CNGB1b is the acceleration of Ca^{2+} influx. The desensitization of A2-A2-A4-B1b channels to cAMP is triggered when Ca^{2+} binds to an endogenous Ca^{2+} sensor that tightly associates with the heteromeric channel complex. Previous work from various laboratories strongly indicates that this endogenous Ca^{2+} sensor is calmodulin, although the final proof is still missing. Endogenous calmodulin is tethered to the native channel protein much more tightly than experimentally applied calmodulin. It can, in fact, be considered an accessory fifth subunit of the A2-A2-A4-B1b channel. Moreover, the channel's response kinetics to exogenous Ca^{2+} calmodulin differ from the Ca^{2+} response of the channel with endogenous calmodulin (the former is biexponential, the latter monoexponential). These differences reflect the temporal properties of two very different binding processes: the association of Ca^{2+} calmodulin to the washed channel versus the association of Ca^{2+} with tethered calmodulin. Our data indicate that the B1b subunit tethers calmodulin but do not reveal the protein domain that stably binds calmodulin to the channel at low Ca^{2+} concentrations. However, the effector site for Ca^{2+}-dependent desensitization is the calmodulin-binding site residing within the N terminus of CNGB1b. Its interaction with tethered calmodulin occurs if either of the two EF-hand domains of calmodulin binds Ca^{2+}. Our peptide experiments suggest that the ability of CNGB1b to bind to partially liganded calmodulin is essential for desensitization. This follows from the finding that the L→E mutation that enables desensitization (Bradley et al., 2004) does not prevent the binding of the peptide to wild-type calmodulin, but only to the mutants CaM^{12} and CaM^{34}, which serve as models for partially liganded calmodulin. Although such peptide data have to be interpreted with caution, this finding is consistent with the notion that one side of the calmodulin molecule is needed for tethering to the channel. The other side is liganded at elevated Ca^{2+} concentrations and interacts with the N-terminal B1b binding site. Desensitization is triggered by this interaction and promotes channel closing at 1–6 µM cAMP. Eventually, the ciliary Ca^{2+} concentration returns to control levels, as Ca^{2+} influx through the desensitized channels ceases and Ca^{2+} is extruded from the ciliary lumen (Reisert and Matthews, 1998). This resets the high cAMP sensitivity of the cAMP-gated channels (Fig. 5 B), preparing the ORN for the next sniff. Thus, calmodulin acts as built-in Ca^{2+} sensor for the A2-A2-A4-B1b channel, located within the Ca^{2+} microdomain at the channel mouth, where it can produce a fast and robust response to inflowing Ca^{2+}. This local feedback mechanism resembles that of other Ca^{2+}-permeable channels, in which Ca^{2+} influx triggers a rapid modulation of gating behavior (Saimi and Kung, 2002; Dunlap, 2007; Tadross et al., 2008).

What is the physiological function of channel desensitization? A recent study of a mouse model in which the CNGB1b calmodulin-binding site was genetically ablated ($CNGB1b^{\Delta CaM}$) has shed light on the function of this feedback inhibition in sensory information processing (Song et al., 2008). Channels in these mice (A2-A2-A4-$B1b^{\Delta CaM}$) have normal cAMP sensitivity, but the ORN response to odor stimuli shows subtle kinetic changes. Surface potential responses of the olfactory epithelium to brief stimuli (electro-olfactograms) show delayed recovery in the $CNGB1b^{\Delta CaM}$ mouse, and responses to

prolonged stimulation display reduced adaptation. The authors suggest that CNGB1b accelerates response termination and, hence, promotes the ORN's ability to respond to consecutive stimuli. Indeed, recordings from the olfactory bulb of CNGB1b$^{\Delta CaM}$ mice yielded evidence for a delayed recovery time in the mutants. Thus, the rapid Ca^{2+}-dependent desensitization of A2-A2-A4-B1b channels may serve to enhance the temporal resolution of signal processing by accelerating response recovery. This interpretation is consistent with the recent finding that odor detection and discrimination is a very fast process (Abraham et al., 2004; Rinberg et al., 2006; Wesson et al., 2008a,b, 2009; Carey et al., 2009). One brief sniff of 100–200-ms duration often suffices for odorant identification. This astonishing rapidity defines a narrow time window for the processes that regulate the activation and desensitization of the A2-A2-A4-B1b channels. Both processes must be effective within ∼100 ms.

Our findings add to the growing body of data that illustrate how ion channels are regulated via constitutively associated calmodulin (Maylie et al., 2004; Fakler and Adelman, 2008; Mori et al., 2008; Tadross et al., 2008). A common theme is the fast regulation by a calmodulin molecule poised in the immediate vicinity of a Ca^{2+}-permeable pore. The stable association of calmodulin with the A2-A2-A4-B1b channel fits to the general concept that sees the fast and transient odor response of an ORN based on the subsecond activation and desensitization of the cAMP-gated channels. Rapid Ca^{2+}-dependent desensitization appears to be a critical aspect of afferent signal generation in the olfactory system.

Summary: the modular organization of olfactory CNG channels

Our data complement the sequential four-step gating model (Biskup et al., 2007) and suggest that olfactory cAMP-gated channels are operated in vivo by three distinct functional modules: (1) a CNGA2 subunit forms the basic gating module that opens the channel; (2) the CNGA4 subunit allows the channel to open at low cAMP concentrations; and (3) the CNGB1b subunit imposes a rapid, Ca^{2+}-dependent feedback control onto the channel. These three functional modules serve to generate a transient receptor current in response to low micromolar concentrations of cAMP during odor stimulation.

We thank Dr. Jonathan Bradley for helpful comments on the manuscript.

K. Vocke prepared the channel mutants; C. Waldeck did the electrophysiology; N. Ungerer prepared the calmodulin mutants and performed the peptide experiments; F. Möhrlen supervised the project; and S. Frings wrote, with the help of all other authors, the manuscript.

This work was supported by the Deutsche Forschungsgemeinschaft (FR 937/7 and MO 1384/1).

Edward N. Pugh Jr. served as editor.

Submitted: 14 July 2009
Accepted: 22 September 2009

REFERENCES

Abraham, N.M., H. Spors, A. Carleton, T.W. Margrie, T. Kuner, and A.T. Schaefer. 2004. Maintaining accuracy at the expense of speed: stimulus similarity defines odor discrimination time in mice. *Neuron*. 44:865–876.

Altenhofen, W., J. Ludwig, E. Eismann, W. Kraus, W. Bönigk, and U.B. Kaupp. 1991. Control of ligand specificity in cyclic nucleotide-gated channels from rod photoreceptors and olfactory epithelium. *Proc. Natl. Acad. Sci. USA*. 88:9868–9872. doi:10.1073/pnas.88.21.9868

Balasubramanian, S., J.W. Lynch, and P.H. Barry. 1996. Calcium-dependent modulation of the agonist affinity of the mammalian olfactory cyclic nucleotide-gated channel by calmodulin and a novel endogenous factor. *J. Membr. Biol.* 152:13–23. doi:10.1007/s002329900081

Bhandawat, V., J. Reisert, and K.W. Yau. 2005. Elementary response of olfactory receptor neurons to odorants. *Science*. 308:1931–1934. doi:10.1126/science.1109886

Biel, M., and S. Michalakis. 2007. Function and dysfunction of CNG channels: insights from channelopathies and mouse models. *Mol. Neurobiol.* 35:266–277. doi:10.1007/s12035-007-0025-y

Biel, M., and S. Michalakis. 2009. Cyclic nucleotide-gated channels. *Handb. Exp. Pharmacol.* 191:111–136.

Biskup, C., J. Kusch, E. Schulz, V. Nache, F. Schwede, F. Lehmann, V. Hagen, and K. Benndorf. 2007. Relating ligand binding to activation gating in CNGA2 channels. *Nature.* 446:440–443. doi:10.1038/nature05596

Bönigk, W., J. Bradley, F. Müller, F. Sesti, I. Boekhoff, G.V. Ronnett, U.B. Kaupp, and S. Frings. 1999. The native rat olfactory cyclic nucleotide-gated channel is composed of three distinct subunits. *J. Neurosci.* 19:5332–5347.

Bradley, J., J. Li, N. Davidson, H.A. Lester, and K. Zinn. 1994. Heteromeric olfactory cyclic nucleotide-gated channels: a subunit that confers increased sensitivity to cAMP. *Proc. Natl. Acad. Sci. USA*. 91:8890–8894. doi:10.1073/pnas.91.19.8890

Bradley, J., D. Reuter, and S. Frings. 2001. Facilitation of calmodulin-mediated odor adaptation by cAMP-gated channel subunits. *Science*. 294:2176–2178. doi:10.1126/science.1063415

Bradley, J., W. Bönigk, K.W. Yau, and S. Frings. 2004. Calmodulin permanently associates with rat olfactory CNG channels under native conditions. *Nat. Neurosci.* 7:705–710. doi:10.1038/nn1266

Bradley, J., J. Reisert, and S. Frings. 2005. Regulation of cyclic nucleotide-gated channels. *Curr. Opin. Neurobiol.* 15:343–349. doi:10.1016/j.conb.2005.05.014

Carey, R.M., J.V. Verhagen, D.W. Wesson, N. Pírez, and M. Wachowiak. 2009. Temporal structure of receptor neuron input to the olfactory bulb imaged in behaving rats. *J. Neurophysiol.* 101:1073–1088. doi:10.1152/jn.90902.2008

Chen, T.Y., and K.W. Yau. 1994. Direct modulation by Ca(2+)-calmodulin of cyclic nucleotide-activated channel of rat olfactory receptor neurons. *Nature.* 368:545–548. doi:10.1038/368545a0

Craven, K.B., and W.N. Zagotta. 2006. CNG and HCN channels: two peas, one pod. *Annu. Rev. Physiol.* 68:375–401. doi:10.1146/annurev.physiol.68.040104.134728

Dhallan, R.S., K.W. Yau, K.A. Schrader, and R.R. Reed. 1990. Primary structure and functional expression of a cyclic nucleotide-activated channel from olfactory neurons. *Nature.* 347:184–187. doi:10.1038/347184a0

Dunlap, K. 2007. Calcium channels are models of self-control. *J. Gen. Physiol.* 129:379–383. doi:10.1085/jgp.200709786

Dzeja, C., V. Hagen, U.B. Kaupp, and S. Frings. 1999. Ca2+ permeation in cyclic nucleotide-gated channels. *EMBO J.* 18:131–144. doi:10.1093/emboj/18.1.131

Fakler, B., and J.P. Adelman. 2008. Control of K(Ca) channels by calcium nano/microdomains. *Neuron.* 59:873–881. doi:10.1016/j.neuron.2008.09.001

Kaupp, U.B., and R. Seifert. 2002. Cyclic nucleotide-gated ion channels. *Physiol. Rev.* 82:769–824.

Keen, J.E., R. Khawaled, D.L. Farrens, T. Neelands, A. Rivard, C.T. Bond, A. Janowsky, B. Fakler, J.P. Adelman, and J. Maylie. 1999. Domains responsible for constitutive and Ca(2+)-dependent interactions between calmodulin and small conductance Ca(2+)-activated potassium channels. *J. Neurosci.* 19:8830–8838.

Kipp, R.A., M.A. Case, A.D. Wist, C.M. Cresson, M. Carrell, E. Griner, A. Wiita, P.A. Albiniak, J. Chai, Y. Shi, et al. 2002. Molecular targeting of inhibitor of apoptosis proteins based on small molecule mimics of natural binding partners. *Biochemistry.* 41:7344–7349. doi:10.1021/bi0121454

Kleene, S.J. 2008. The electrochemical basis of odor transduction in vertebrate olfactory cilia. *Chem. Senses.* 33:839–859. doi:10.1093/chemse/bjn048

Kurahashi, T., and A. Menini. 1997. Mechanism of odorant adaptation in the olfactory receptor cell. *Nature.* 385:725–729. doi:10.1038/385725a0

Liman, E.R., and L.B. Buck. 1994. A second subunit of the olfactory cyclic nucleotide-gated channel confers high sensitivity to cAMP. *Neuron.* 13:611–621. doi:10.1016/0896-6273(94)90029-9

Liu, M.Y., T.Y. Chen, B. Ahamed, J. Li, and K.W. Yau. 1994. Calcium-calmodulin modulation of the olfactory cyclic nucleotide-gated cation channel. *Science.* 266:1348–1354. doi:10.1126/science.266.5189.1348

Lynch, J.W., and B. Lindemann. 1994. Cyclic nucleotide-gated channels of rat olfactory receptor cells: divalent cations control the sensitivity to cAMP. *J. Gen. Physiol.* 103:87–106. doi:10.1085/jgp.103.1.87

Matulef, K., and W.N. Zagotta. 2003. Cyclic nucleotide-gated ion channels. *Annu. Rev. Cell Dev. Biol.* 19:23–44. doi:10.1146/annurev.cellbio.19.110701.154854

Maylie, J., C.T. Bond, P.S. Herson, W.S. Lee, and J.P. Adelman. 2004. Small conductance Ca2+-activated K+ channels and calmodulin. *J. Physiol.* 554:255–261. doi:10.1113/jphysiol.2003.049072

Mori, M.X., C.W. Vander Kooi, D.J. Leahy, and D.T. Yue. 2008. Crystal structure of the CaV2 IQ domain in complex with Ca2+/calmodulin: high-resolution mechanistic implications for channel regulation by Ca2+. *Structure.* 16:607–620. doi:10.1016/j.str.2008.01.011

Munger, S.D., A.P. Lane, H. Zhong, T. Leinders-Zufall, K.W. Yau, F. Zufall, and R.R. Reed. 2001. Central role of the CNGA4 channel subunit in Ca2+-calmodulin-dependent odor adaptation. *Science.* 294:2172–2175. doi:10.1126/science.1063224

Nache, V., E. Schulz, T. Zimmer, J. Kusch, C. Biskup, R. Koopmann, V. Hagen, and K. Benndorf. 2005. Activation of olfactory-type cyclic nucleotide-gated channels is highly cooperative. *J. Physiol.* 569:91–102. doi:10.1113/jphysiol.2005.092304

Owenius, R., M. Osterlund, M. Lindgren, M. Svensson, O.H. Olsen, E. Persson, P.O. Freskgård, and U. Carlsson. 1999. Properties of spin and fluorescent labels at a receptor-ligand interface. *Biophys. J.* 77:2237–2250. doi:10.1016/S0006-3495(99)77064-5

Patton, C., S. Thompson, and D. Epel. 2004. Some precautions in using chelators to buffer metals in biological solutions. *Cell Calcium.* 35:427–431.

Peng, C., E.D. Rich, and M.D. Varnum. 2004. Subunit configuration of heteromeric cone cyclic nucleotide-gated channels. *Neuron.* 42:401–410. doi:10.1016/S0896-6273(04)00225-9

Peterson, B.Z., C.D. DeMaria, J.P. Adelman, and D.T. Yue. 1999. Calmodulin is the Ca2+ sensor for Ca2+-dependent inactivation of L-type calcium channels. *Neuron.* 22:549–558. doi:10.1016/S0896-6273(00)80709-6

Pifferi, S., A. Boccaccio, and A. Menini. 2006. Cyclic nucleotide-gated ion channels in sensory transduction. *FEBS Lett.* 580:2853–2859. doi:10.1016/j.febslet.2006.03.086

Qu, W., A.J. Moorhouse, M. Chandra, K.D. Pierce, T.M. Lewis, and P.H. Barry. 2006. A single P-loop glutamate point mutation to either lysine or arginine switches the cation-anion selectivity of the CNGA2 channel. *J. Gen. Physiol.* 127:375–389. doi:10.1085/jgp.200509378

Reisert, J., and H.R. Matthews. 1998. Na^+-dependent Ca^{2+} extrusion governs response recovery in frog olfactory receptor cells. *J. Gen. Physiol.* 112:529–535. doi:10.1085/jgp.112.5.529

Rinberg, D., A. Koulakov, and A. Gelperin. 2006. Speed-accuracy tradeoff in olfaction. *Neuron.* 51:351–358. doi:10.1016/j.neuron.2006.07.013

Saimi, Y., and C. Kung. 2002. Calmodulin as an ion channel subunit. *Annu. Rev. Physiol.* 64:289–311. doi:10.1146/annurev.physiol.64.100301.111649

Sautter, A., X. Zong, F. Hofmann, and M. Biel. 1998. An isoform of the rod photoreceptor cyclic nucleotide-gated channel beta subunit expressed in olfactory neurons. *Proc. Natl. Acad. Sci. USA.* 95:4696–4701. doi:10.1073/pnas.95.8.4696

Shapiro, M.S., and W.N. Zagotta. 2000. Structural basis for ligand selectivity of heteromeric olfactory cyclic nucleotide-gated channels. *Biophys. J.* 78:2307–2320. doi:10.1016/S0006-3495(00)76777-4

Song, Y., K.D. Cygnar, B. Sagdullaev, M. Valley, S. Hirsh, A. Stephan, J. Reisert, and H. Zhao. 2008. Olfactory CNG channel desensitization by Ca2+/CaM via the B1b subunit affects response termination but not sensitivity to recurring stimulation. *Neuron.* 58:374–386. doi:10.1016/j.neuron.2008.02.029

Tadross, M.R., I.E. Dick, and D.T. Yue. 2008. Mechanism of local and global Ca2+ sensing by calmodulin in complex with a Ca2+ channel. *Cell.* 133:1228–1240. doi:10.1016/j.cell.2008.05.025

Takeuchi, H., and T. Kurahashi. 2005. Mechanism of signal amplification in the olfactory sensory cilia. *J. Neurosci.* 25:11084–11091. doi:10.1523/JNEUROSCI.1931-05.2005

Tibbs, G.R., D.T. Liu, B.G. Leypold, and S.A. Siegelbaum. 1998. A state-independent interaction between ligand and a conserved arginine residue in cyclic nucleotide-gated channels reveals a functional polarity of the cyclic nucleotide binding site. *J. Biol. Chem.* 273:4497–4505. doi:10.1074/jbc.273.8.4497

Trudeau, M.C., and W.N. Zagotta. 2003. Calcium/calmodulin modulation of olfactory and rod cyclic nucleotide-gated ion channels. *J. Biol. Chem.* 278:18705–18708. doi:10.1074/jbc.R300001200

Varnum, M.D., K.D. Black, and W.N. Zagotta. 1995. Molecular mechanism for ligand discrimination of cyclic nucleotide-gated channels. *Neuron.* 15:619–625. doi:10.1016/0896-6273(95)90150-7

Weitz, D., M. Zoche, F. Müller, M. Beyermann, H.G. Körschen, U.B. Kaupp, and K.W. Koch. 1998. Calmodulin controls the rod photoreceptor CNG channel through an unconventional binding site in the N-terminus of the beta-subunit. *EMBO J.* 17:2273–2284. doi:10.1093/emboj/17.8.2273

Weitz, D., N. Ficek, E. Kremmer, P.J. Bauer, and U.B. Kaupp. 2002. Subunit stoichiometry of the CNG channel of rod photoreceptors. *Neuron.* 36:881–889. doi:10.1016/S0896-6273(02)01098-X

Wesson, D.W., R.M. Carey, J.V. Verhagen, and M. Wachowiak. 2008a. Rapid encoding and perception of novel odors in the rat. *PLoS Biol.* 6:e82. doi:10.1371/journal.pbio.0060082

Wesson, D.W., T.N. Donahou, M.O. Johnson, and M. Wachowiak. 2008b. Sniffing behavior of mice during performance in odor-guided tasks. *Chem. Senses.* 33:581–596. doi:10.1093/chemse/bjn029

Wesson, D.W., J.V. Verhagen, and M. Wachowiak. 2009. Why sniff fast? The relationship between sniff frequency, odor discrimination, and receptor neuron activation in the rat. *J. Neurophysiol.* 101:1089–1102. doi:10.1152/jn.90981.2008

Williams, D.A., and F.S. Fay. 1990. Intracellular calibration of the fluorescent calcium indicator Fura-2. *Cell Calcium.* 11:75–83. doi:10.1016/0143-4160(90)90061-X

Zheng, J., and W.N. Zagotta. 2004. Stoichiometry and assembly of olfactory cyclic nucleotide-gated channels. *Neuron.* 42:411–421. doi:10.1016/S0896-6273(04)00253-3

Zheng, J., M.C. Trudeau, and W.N. Zagotta. 2002. Rod cyclic nucleotide-gated channels have a stoichiometry of three CNGA1 subunits and one CNGB1 subunit. *Neuron.* 36:891–896. doi:10.1016/S0896-6273(02)01099-1

Zheng, J., M.D. Varnum, and W.N. Zagotta. 2003. Disruption of an intersubunit interaction underlies Ca2+-calmodulin modulation of cyclic nucleotide-gated channels. *J. Neurosci.* 23:8167–8175.

Zhong, H., L.L. Molday, R.S. Molday, and K.W. Yau. 2002. The heteromeric cyclic nucleotide-gated channel adopts a 3A:1B stoichiometry. *Nature.* 420:193–198. doi:10.1038/nature01201

Waldeck et al., http://www.jgp.org/cgi/content/full/jgp.200910296/DC1

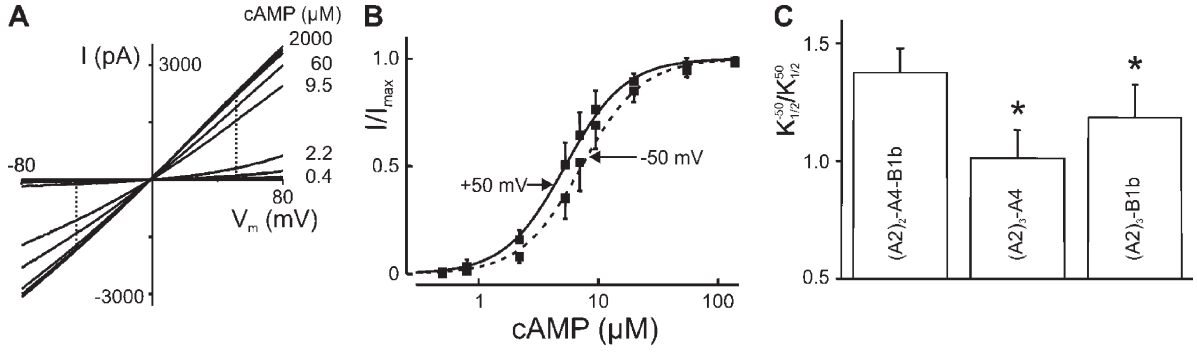

Figure S1. Voltage dependence of $K_{1/2}^{cAMP}$ as criterion for A2-A2-A4-B1b coassembly. In patches with predominant A2-A2-A4-B1b channel activity, I/V_m relations displayed a slight but distinct voltage dependence of $K_{1/2}^{cAMP}$, the cAMP concentration for half-maximal channel activation. (A) A family of I/V_m relations recorded at the indicated cAMP concentrations from a patch with predominant A2-A2-A4-B1b expression. To determine $K_{1/2}^{cAMP}$, I/I_{max} was measured for each cAMP concentration at −50 and +50 mV (dotted lines). (B) Dependence of I/I_{max} on cAMP concentration at −50 and +50 mV. Hill-type functions fitted to mean data from seven patches yielded $K_{1/2}^{cAMP}$ = 7.3 ± 1.7 μM, n = 1.71 ± 0.3, for −50 mV (dashed line), and $K_{1/2}^{cAMP}$ = 5.3 ± 1.2 μM, n = 1.73 ± 0.3, for +50 mV (solid line). (C) The ratio of $K_{1/2}$ values measured at −50 and +50 mV ($K_{1/2}^{-50}$ / $K_{1/2}^{+50}$) was determined for patches with predominant A2-A2-A4-B1b expression (1.38 ± 0.1; seven patches) for cells transfected with CNGA2 and CNGA4 (1.01 ± 0.1; four patches), and for cells transfected with CNGA2 and CNGB1b (1.18 ± 0.13; four patches). The $K_{1/2}^{-50}$ / $K_{1/2}^{+50}$ values for A2-A2-A2-A4 and for A2-A2-A2-B1b channels are significantly different ($P < 0.001$ and 0.05, respectively) from the A2-A2-A4-B1b value. Thus, $K_{1/2}^{-50}$ / $K_{1/2}^{+50}$ values >1.3 can be used as a criterion for A2-A2-A4-B1b expression.

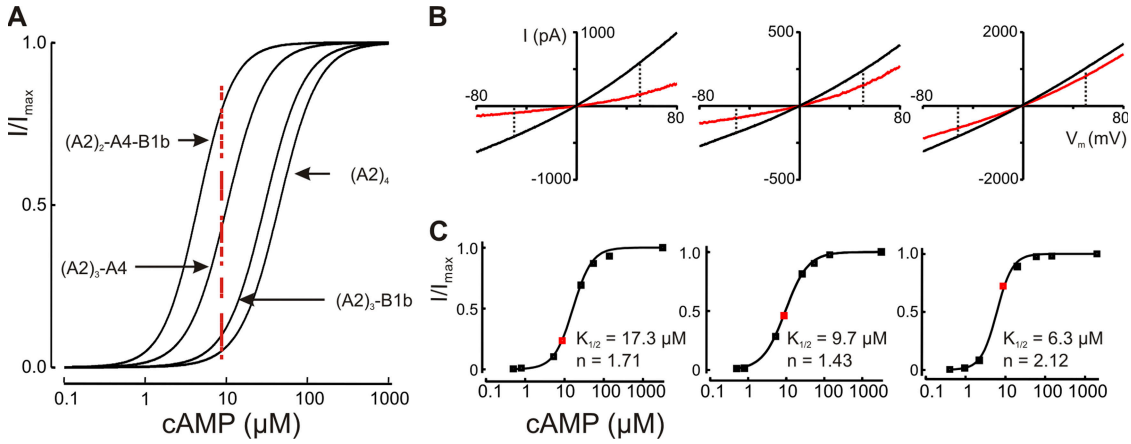

Figure S2. Coassembly of CNGA2, CNGA4, and CNGB1b in HEK 293 cells. HEK 293 cells were transfected with CNGA2, CNGA4, and CNGB1b, and the cAMP sensitivity of the expressed channel was used to assay their subunit composition. We used the cAMP concentration for half-maximal channel activation, $K_{1/2}$, which has a characteristic value, determined for each subunit combination by single-channel analysis (Bönigk et al. 1999. *J. Neurosci.* 19:5332-5347). In experiments with only two different subunits, the measured $K_{1/2}$ values were close to the ones expected for A2-A2-A2-A4 or A2-A2-A2-B1b channels, indicating that only a negligible fraction of A2 homomers was present in the patches. However, when all three subunits were coexpressed, channels with different subunits were present in the patches. To identify patches with predominant A2-A2-A4-B1b expression, we derived a test parameter from the following consideration. If channels with different subunit compositions are active in the same patch, the relative current, I/I_{max}, depends on the weighted sum of four Hill-type relations, each of which describes the cAMP dependence of one specific subunit combination:

$$I / I_{max} = x_1 H_1(\mathrm{A2-A2-A4-B1b}) + x_2 H_2(\mathrm{A2-A2-A2-A4}) + x_3 H_3(\mathrm{A2-A2-A2-B1b}) + x_4 H_4(\mathrm{A2})$$

In this equation, H_i represents the Hill term, $c^n/(c^n + K_{1/2}^n)$, for one specific subunit combination, and x_i is a corresponding scaling factor. The two parameters $K_{1/2}$ and n were taken from single-channel recordings with known subunit combinations (Bönigk et al. 1999. *J. Neurosci.* 19:5332-5347). The values are 40 μM and 2.5 for A2 homomers, 28 μM and 1.9 for A2-A2-A2-B1b, and 4 μM and 2.0 for A2-A2-A4-B1b (stoichiometries determined by Zheng et al. [2004. *Neuron.* 42:411–421]). The values for A2-A2-A2-A4 (10 μM and 1.8) were obtained from macroscopic currents, as single-channel analysis was not feasible (Bönigk et al. 1999. *J. Neurosci.* 19:5332-5347). We used test solutions containing either 3.4 or 9 μM cAMP. For these cAMP concentrations, our analysis predicts that the relative current recorded from a patch with predominant A2-A2-A4-B1b expression ($x_1/[x_2+x_3+x_4] > 10$) would be >0.31 and >0.63, respectively. We used patches for the A2-A2-A4-B1b experiments only if I/I_{max} exceeded these values because the patches contained <10% of channels with subunit combinations different from A2-A2-A4-B1b. (A) To illustrate the heterogeneity of subunit assembly, I/I_{max} values from 66 patches at 9 μM cAMP (red dots) are shown together with the dose–response relations of all functional subunit combinations. (B) I/V_m relations and (C) corresponding dose–response relations of three representative patches with I/I_{max} values of 0.23, 0.45, and 0.72 demonstrate the necessity to select patches with predominant A2-A2-A4-B1b expression. Only the patch shown on the right displayed the specific values of $K_{1/2}$ and n characteristic for A2-A2-A4-B1b channels on the basis of single-channel analysis. The other patches contained >10% of other subunit combinations, resulting in reduced cAMP sensitivity (larger $K_{1/2}$ values) and reduced cooperativity of channel gating (smaller n values).

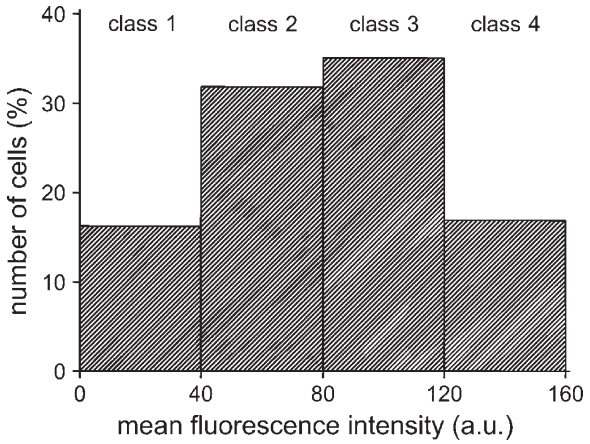

Figure S3. Classification of cells with different expression levels of CNGA2^{YFP}. HEK 293 cells were transfected with pcDNA3.1^{+}/*CNGA2*^{YFP}. 48 h after transfection, cells were transferred to an epifluorescence microscope. Cells were imaged (λ_{exc} = 490 nm; λ_{em} = 510 nm) with identical camera settings, and the mean pixel intensity was determined for each cell. Fluorescence of nontransfected cells was subtracted as background. The fluorescence values of all cells were divided into four classes according to the histogram shown. Only class 4 cells were used for the patch clamp experiments. Analysis of cAMP-gated channels in cells with different channel densities did not reveal any difference in channel properties, indicating that channel assembly worked similarly in all four cell classes.

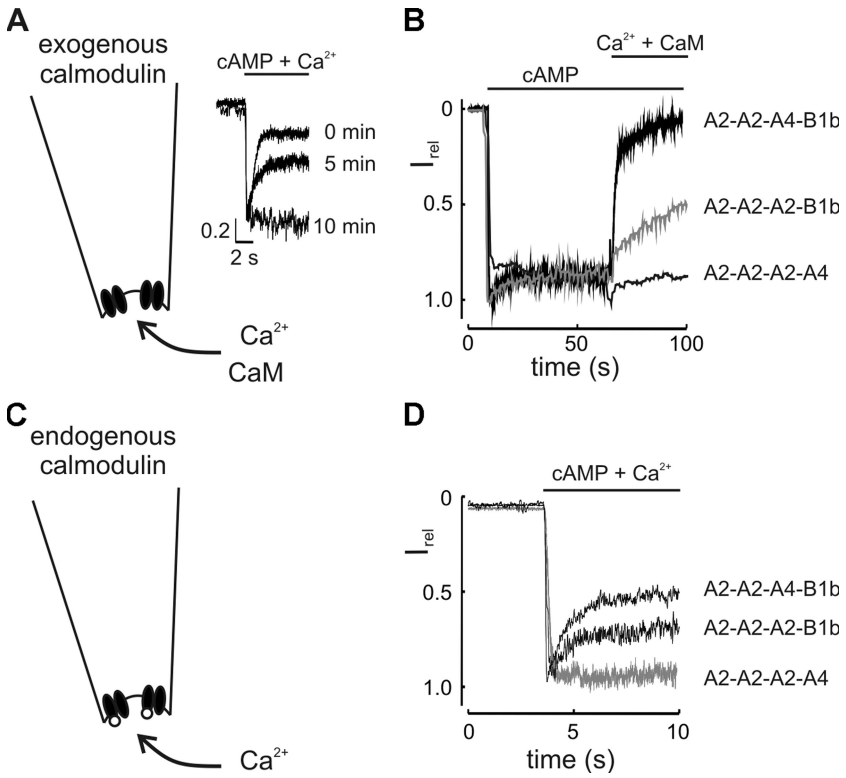

Figure S4. Endogenous and exogenous channel–calmodulin complexes. As shown previously (Bradley et al. 2001. *Science.* 294:2176-2178; Bradley et al. 2004. *Nat. Neurosci.* 7:705-710), calmodulin causes rapid desensitization in A2-A2-A4-B1b channels when added to washed channels in excised patches (exogenous complex). Desensitization is much slower when either CNGA4 or CNGB1b are absent. In contrast, the endogenous channel–calmodulin complex that forms within the cell does not require CNGA4, but it depends on the presence of CNGB1b. (A) Protocol to set up the exogenous complex. A patch with cAMP-gated channels was excised from a transfected cell and exposed to Ca^{2+}-free solution (with 10 mM EGTA) for 10 min. During this time, the channels progressively lost Ca^{2+} sensitivity (inset) as their endogenous calmodulin was washed away. (B) Response of washed cAMP-gated channels to the application of 150 µM Ca^{2+}/0.5 µM calmodulin during activation by cAMP. A2-A2-A4-B1b channels showed rapid current decline at 15 µM cAMP due to desensitization by the exogenous channel–calmodulin complex. A much slower response was seen with A2-A2-A2-A4 channels at 30 µM cAMP and with A2-A2-A2-B1b channels at 40 µM cAMP. (C) To preserve the endogenous association of calmodulin with the channel, patches were excised from transfected HEK 293 cells into a solution that contained 2.5 mM Ca^{2+}. (D) After a brief exposure to Ca^{2+}-free solution, the current recordings at −50 mV show the channel response to 20 µM Ca^{2+}, mediated by the endogenous calmodulin–channel complex. Both A2-A2-A4-B1b and A2-A2-A2-B1b channels responded rapidly (note different time scale), whereas A2-A2-A2-A4 channels did not display any desensitization.

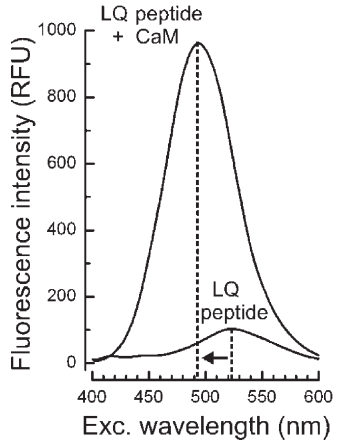

Figure S5. Fluorescence readout for BADAN-labeled LQ peptide of CNGB1b. To monitor the interaction of calmodulin with a 26-residue peptide that comprises the LQ consensus site for calmodulin binding (LQ peptide), the peptide was labeled with BADAN, which was excited at 387 nm. Fluorescence emission increased upon calmodulin binding, and the fluorescence peak shifted from 520 to 490 nm (arrow). This shift was used to monitor peptide–calmodulin binding.